

Revisiting Multi-User Downlink in IEEE 802.11ax: A Designers Guide to MU-MIMO

Liu Cao, Lyutianyang Zhang, Sumit Roy, *Fellow, IEEE*, Sian Jin

Abstract—Downlink (DL) Multi-User (MU) Multiple Input Multiple Output (MU-MIMO) is a key technology that allows multiple concurrent data transmissions from an Access Point (AP) to a selected sub-set of clients for higher network efficiency in IEEE 802.11ax. However, DL MU-MIMO feature is typically turned off as the default setting in AP vendors’ products, that is, turning on the DL MU-MIMO may not help increase the network efficiency, which is counter-intuitive. In this article, we provide a sufficiently deep understanding of the interplay between the various underlying factors, i.e., CSI overhead and spatial correlation, which result in negative results when turning on the DL MU-MIMO. Furthermore, we provide a fundamental guideline as a function of operational scenarios to address the fundamental question “when the DL MU-MIMO should be turned on/off”.

Index Terms—IEEE 802.11ax, Downlink, MU-MIMO, CSI overhead, Spatial correlation

I. INTRODUCTION

IEEE 802.11ax (Wi-Fi 6) marked a significant evolution milestone via the introduction of Multi-User (MU) communication modes (in contrast with legacy Single-User (SU) communication) for both Uplink (UL) and Downlink (DL) in tri-band (2.4/5/6 GHz) [1]. For the Uplink, this implies the use of trigger-based OFDMA; in this article, we focus solely on DL Multi-User (MU) Multiple Input Multiple Output (MU-MIMO). Legacy Single-User MIMO (SU-MIMO) - the precursor to MU-MIMO - laid the groundwork by allowing transmission of multiple spatial streams from an access point (AP) equipped with multiple antennas to a single client device on downlink. With the proliferation of wireless client devices, a single Wi-Fi network access point (AP) can have many (typically 10–20) associated stations (STAs) [2], [3]. With multi-antenna clients¹, it is feasible via DL Transmit Beamforming (TxBF) at the AP to send multiple streams to multiple STAs simultaneously (DL MU-MIMO).

A typical configuration [4], [5] such as Fig. 1 assumes an 8 x 8 AP (e.g., NetGear RAXE500) and 2 x 2 STAs (e.g., iPhone 15 and MacBook Air), implying that a single downlink transmission opportunity can potentially send a total of 8 spatial streams² to a selected sub-set of clients (e.g.

Liu Cao, Lyutianyang Zhang and Sumit Roy are with the Department of Electrical & Computer Engineering, University of Washington, Seattle, WA, USA (e-mail: {liucaoc, lyutiz, sroy}@uw.edu). Sian Jin is with MathWorks, Natick, MA, USA (e-mail: sianjin@mathworks.com). (*Corresponding author: Lyutianyang Zhang*)

¹However, the number of antennas at the AP always exceeds the number of antennas at a client.

²Note that Wi-Fi 5 (IEEE 802.11ac) included support for MU-MIMO but limited to 4 streams on only 5 GHz downlink operation; whereas Wi-Fi 6 supports up to 8-stream on 2.4/5/6 GHz uplink/downlink operations.

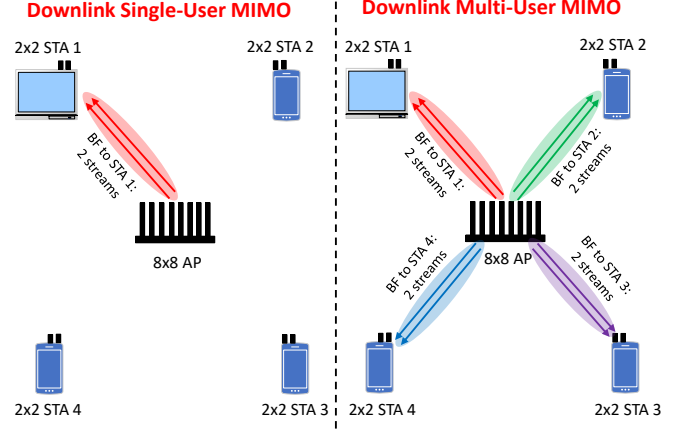


Fig. 1: SU-MIMO vs MU-MIMO on Downlink Operations.

2 streams each to 4 STAs). While DL SU-MIMO results in scaling of per-user throughput as a result of multi-stream transmission, its benefits are limited by the fact that most clients support either 1 or 2 spatial streams (i.e., a total of 2-stream transmissions in DL SU-MIMO in Fig. 1). By contrast, it is evident that in dense overlapped network scenarios - such as the enterprise or residential cluster - DL MU-MIMO provides a natural pathway to increasing network efficiency (aggregate network throughput) by *enabling simultaneous transmissions of multiple streams to multiple clients* (i.e., a total of 8-stream transmissions in DL MU-MIMO in Fig. 1), with appropriate choice of the user sub-set and TxBF to minimize inter-user/inter-stream interference.

Despite the promise of MU-MIMO for improved network capacity via simultaneous transmission to multiple users on downlink³, real-world user testing has revealed significant challenges. A noticeable discrepancy exists between the theoretical speeds advertised by manufacturers who incorporate DL MU-MIMO and the actual throughput measured in specific conditions [6]–[8]. An industry test report [9] showed that turning on MU-MIMO resulted in 58% aggregate throughput loss compared to SU-MIMO when pairing 4 x 4 Broadcom-based router with 2 x 2 Qualcomm-based STAs. An earlier research study [10] demonstrated that DL SU-MIMO achieves 16.8% to 42% higher aggregated throughput MU-MIMO based on a test of a commercial 4 x 4 MU-MIMO-capable 802.11ac 5 GHz radio with 1 x 1 Xiaomi Mi 4i smartphones. Such variation in results is attributable to various factors at play,

³There exists an analogous feature for the uplink: trigger-based OFDMA whereby a 20 MHz channel may be shared synchronously by multiple users. However, consideration of UL OFDMA is beyond the scope of this article.

including the complex interplay of channel state information (CSI) overhead, device capabilities and environmental (propagation) conditions as a function of user location. In this article, we chose the IEEE 802.11ax indoor channel model [11], widely used by the industry and academia, for a foundational exploration of DL SU/MU-MIMO throughput. Specifically, as the selected sub-set of clients for MU-MIMO on downlink are closer to each other in dense networks, increased spatial correlation will lead to significant inter-user and inter-stream interference in DL MU-MIMO. Thus overall network throughput degrades unless counteracted by a combination of inter-user interference cancellation and user selection algorithms [12], [13]. Moreover, CSI overhead affects both SU and MU aggregate throughput; in particular, CSI overhead increases significantly with the dimensionality of MU-MIMO. In turn, this implies that any MU-MIMO design must carefully consider the issue of (optimal) channel sounding periodicity when confronted with channel time variations⁴.

The lack of a sufficiently deep understanding of the interplay between the various underlying factors discussed has resulted in AP vendors turning off the DL MU-MIMO feature as default setting in their products, reflecting the current ambivalence surrounding DL MU-MIMO. The primary purpose of this article is therefore to provide *new insights underlying the fundamental question: “when should DL MU-MIMO be turned on/off”* as a function of the operational scenario. By a combination of analysis and computation/simulation, we attempt to answer the above question by

- Identifying set of conditions where DL SU-MIMO outperforms MU-MIMO and vice-versa;
- Provide broad ‘rules of thumb’ regarding use of DL MU-MIMO in current/future Wi-Fi systems.

The rest of this article is organized as follows. Section II introduces the impact of DL SU and MU CSI overhead differences on their effective channel capacity; In Section III, we explore the impact of spatial correlation on the MU channel capacity under the IEEE 802.11ax indoor channel model. In Section IV, a design guideline table for DL MU-MIMO is proposed by unifying the factors discussed in Section II and III. Finally, Section V concludes this article.

II. FACTOR 1: CSI OVERHEAD

In 802.11ax DL transmission, AP is the transmitter which is called the beamformer, while a STA is the receiver which is called the beamformee. Beamforming depends on channel calibration procedures, called channel sounding in the 802.11ax standard. The channel sounding allows the beamformer to gather the beamforming report(s) that characterize the beamformee location(s) and to transmit the streams toward the precise direction of the beamformee(s).

A. DL SU/MU-MIMO channel sounding

DL SU-MIMO is indicated by feedback type 0 in the High-Efficiency (HE) MIMO control field. As Fig. 2 shows, its channel sounding process consists of four major steps:

- The beamformer begins the process by broadcasting a Null Data Packet Announcement (NDPA) frame, which is used to gain control of the channel and identify the intended beamformee.
- The beamformer next transmits a Null Data Packet (NDP) to beamformee after a Short Interframe Space (SIFS). NDP is an empty frame that only contains the Physical Layer Protocol Data Unit (PPDU) header. The received NDP is used for channel estimation by analyzing the OFDM training symbols, called HE-LTF, whose length is a variable that depends on the number of spatial streams.
- Following receipt of the NDP, the beamformee responds with a BF feedback matrix in a compressed form. The BF feedback matrix instructs how the beamformer should steer the data frame to the beamformee with higher energy. Codebook information in the HE MIMO Control field provides the resolution schemes for compressing the BF feedback matrix.
- The beamformer receives and recovers the compressed feedback matrix that is further used as the steering matrix to direct HE data transmissions toward the beamformee.

By contrast, DL MU-MIMO, indicated by feedback type 1 in the HE MIMO control field, follows the similar channel sounding protocols as the SU-MIMO, however, several **major** differences exist:

- NDPA frame format: A HE NDPA frame in MU-MIMO includes multiple STA Info fields, one for each beamformee, while the NDPA frame in SU-MIMO only carries a single STA Info field.
- BF Report Poll (BFRP) trigger frame: The compressed BF feedback in SU-MIMO comes right after the NDP. However, the beamformer in DL MU-MIMO must use a control frame - BFRP Trigger frame that instructs each beamformees to transmit the BF feedback simultaneously. The AP may transmit other BFRP Trigger frames to gather more feedbacks if necessary.
- Compressed BF feedback frame format: The HE MU Exclusive BF report is an extra field at the end of the frame for MU-MIMO, which thereby introduce extra CSI overhead;
- BF Feedback transmission: The BF feedback in SU-MIMO is transmitted over the UL OFDM while they are transmitted over the UL OFDMA in MU-MIMO.

B. CSI Overhead Comparison

CSI overhead in DL SU/MU-MIMO can be calculated based on the CSI frame format indicating each sub-field size, as shown in Fig. 2. In particular, CSI overhead is dominated by HE compressed BF feedback that contains the HE compressed BF report (as well as the extra sub-field - HE MU Exclusive BF report in MU-MIMO). The compressed BF report contains the compressed CSI for each sub-carrier, i.e., the **V-matrix** or

⁴Further consideration of this topic is beyond the scope of this article.

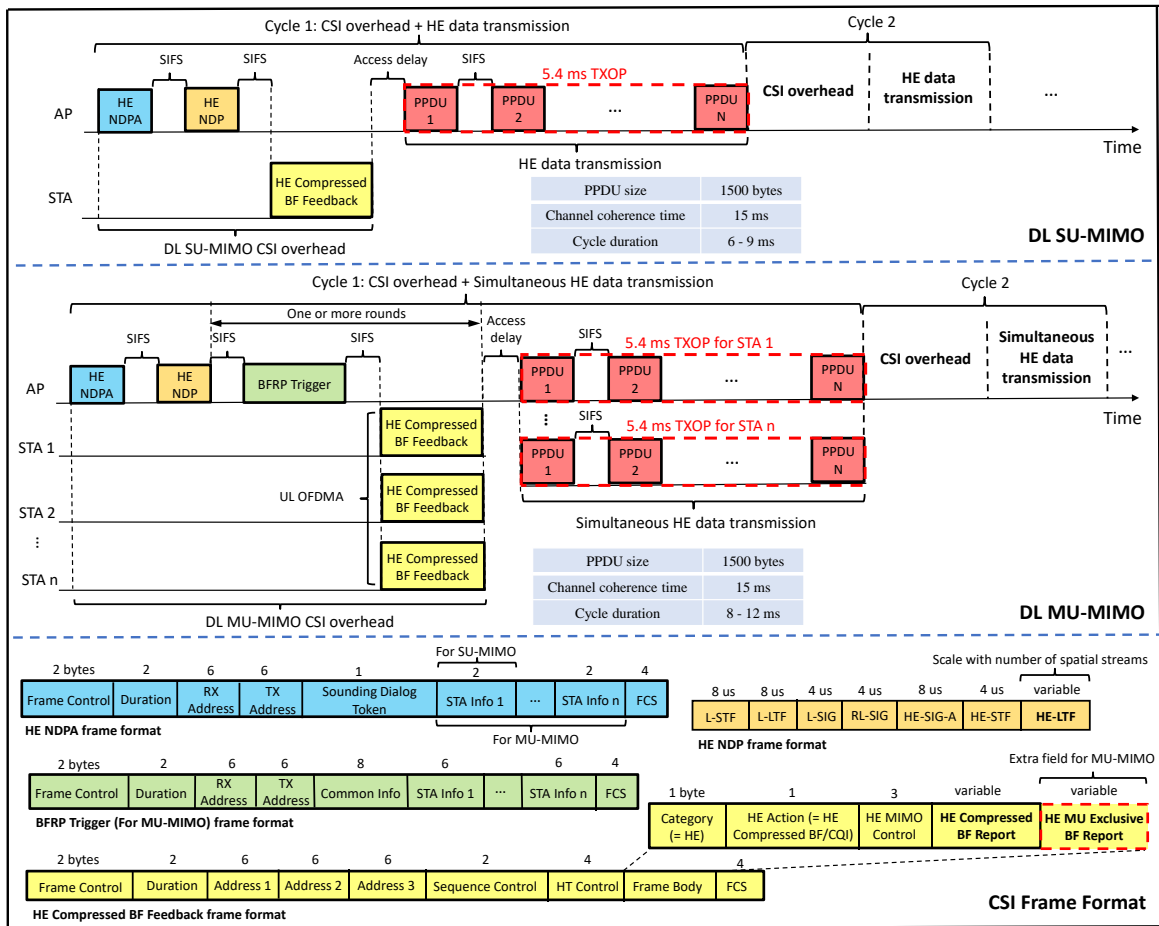


Fig. 2: IEEE 802.11ax Channel Sounding followed by High-Efficiency (HE) Data Transmission.

steering/precoding matrix⁵ used for digital beamforming. V-matrix is obtained by a) applying the singular value decomposition (SVD) to the full CSI, and b) compressing it to specific Givens rotation angles to reduce the amount of required bits. The compressed size of the V-matrix depends on the total number of Givens rotation angles as well as the number of bits used to quantize each angle, as defined in IEEE 802.11ax specification. In general, the larger the V-matrix dimension, the more the number of angles. Meanwhile, the number of bits to quantize each angle is indicated by the sub-field of codebook information choice with 1 bit in the HE MIMO Control field. Thus both SU- and MU- have two codebook information choices [1], however, MU-MIMO uses more bits than SU-MIMO to quantize a single angle by using the same codebook information. For instance, if codebook information bit is set to 0, the number of bits to quantize an angle in SU-MIMO is 4 or 2 while they are 7 or 5 in MU-MIMO [1], implying that the compressed V-matrix in MU-MIMO has larger overhead compared to SU-MIMO. In addition, the HE compressed BF report size also scales with the number of spatial streams and

the number of sub-carriers. The MU-Exclusive BF report in MU-MIMO contains the delta SNR per sub-carrier, which represents the difference from the average SNR. The MU-Exclusive BF report represents the spatial characteristics for each sub-carrier caused by the environment, the size of which scales with the number of subcarriers. Since the 802.11ax specification does not detail how this information is exploited in the design of the beamformer, its implementation is chip vendor dependent.

As discussed, channel sounding procedures introduce a significant cost in airtime because the sounding exchange must be completed before a beamformed data transmission can occur. Therefore, if the MU-MIMO BF gain is not sufficient to offset the airtime consumed by the sounding exchange, MU-MIMO throughput can be lower than the SU-MIMO in some operational scenarios.

As Fig. 2 shows, a cycle of CSI overhead and HE data transmission is repeated in both DL SU and MU-MIMO. In each cycle, the transmitted data for each STA is filled in one Transmit opportunity (TXOP) comprised of multiple back-to-back PPDU (e.g., 1500 bytes) in SIFS burst mode. Thus the data transmission duration is the maximum TXOP limit (5.4 ms) compared to which the duration of access delay is negligible (typically less than a few hundred microseconds), as long as the number of STAs is not excessively large. If

⁵The Null-steering step based on zero-forcing (ZF) and minimum mean square error (MMSE) approaches [12], [14], used for precoding in DL MU-MIMO are not implemented in real AP products [7], [10] because those can be implemented only if the full CSI is obtained, whereas the feedback V-matrix provides only partial CSI. Besides, null-steering step incurs additional computational complexity and thus chipset cost for the AP.

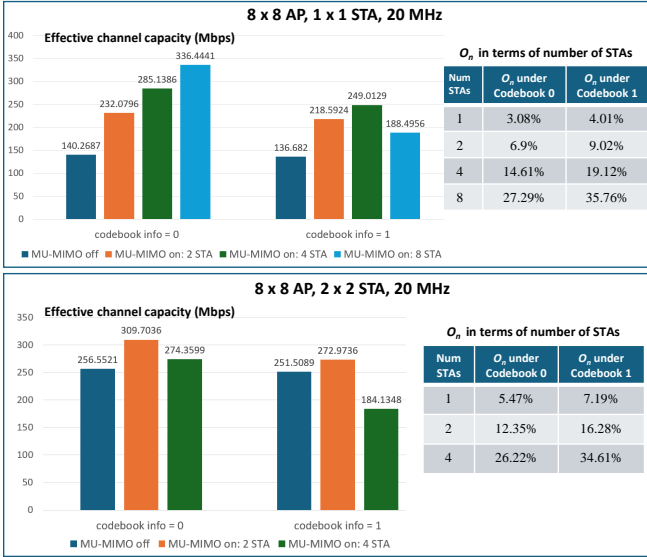


Fig. 3: Effective Channel Capacity impacted by CSI Overhead. Average 25 dB SNR at the single STA in SU-MIMO.

we assume STA's walking speed equal to 2 mph, the resulting channel coherence time⁶ (15 ms) will be greater than any one cycle duration. Hence, it is reasonable to assume a block fading channel for each cycle, i.e., channel capacity is fixed in a cycle while varying across different cycles. We will use the *effective channel capacity* C_{eff} to compare the SU and MU- performance as a function of CSI overhead - defined as the average channel capacity over both CSI overhead (zero channel capacity) duration and HE data transmission duration (non-zero channel capacity), given by

$$C_{\text{eff}} = \frac{1}{N} \sum_{n,k} (1 - O_n) \cdot C_{n,k}, \quad (1)$$

where N denotes the total number of cycles, $C_{n,k}$ denotes the Shannon channel capacity [14] of the k -th STA in the n -th cycle, assumed to be constant due to the block fading channel. O_n is the ratio of CSI overhead airtime to the cycle duration for the n -th cycle. Eq. (1) applies to DL SU-MIMO when the size of k is 1. Note that $C_{n,k}$ varies across n due to time-varying channels⁷, but O_n is independent of n in our model since we assume a specific setup (i.e., MIMO dimension, codebook information, and the number of selected STAs, TXOP duration).

Assuming the 8 x 8 AP, 1 x 1 STA and 20 MHz (242 sub-carriers) bandwidth as in Fig. 3, the effective channel capacity does *not* grow linearly with the number of STAs. In particular, the effective channel capacity under codebook info 1 is greatly reduced when the number of STAs reaches 8. This can be explained by following reasons:

⁶Channel coherence time is defined as the time duration over which the channel is considered to be not varying.

⁷For the pure analysis of CSI overhead in this section, the inter-user interference determined by spatial correlation is assumed to be zero. Thus $C_{n,k}$ in terms of n changes only due to the channel gain variations rather than variations in inter-user interference. Then, C_{eff} shown in Fig. 3 is the maximum effective channel capacity that DL MU-MIMO can reach.

- CSI overhead proportion O_n shown in Fig. 3 grows exponentially with the number of STAs. This is because, on the one hand, an extra field - HE MU Exclusive BF report as a function of the number of sub-carriers and spatial streams - is included in HE compressed BF feedback, incurring extra CSI overhead; On the other hand, the bandwidth is shared using UL OFDMA leads to the lower UL data rate for HE compressed BF feedback transmission per STA; Thus, the DL MU-MIMO CSI overhead becomes significantly higher than SU-MIMO for a large number of STAs;
- AP transmit power is divided equally for each STA in DL MU-MIMO. As a result, $C_{n,k}$ in Eq. (1) will drop with increasing number of STAs due to the lower transmit power per STA.

The same phenomenon repeats for the 8 x 8 AP, 2 x 2 STA, and 20 MHz cases in Fig. 3; the effective channel capacity is reduced when the number of STAs reaches 4. However, this does not indicate that AP shall not support more STAs due to the lower effective channel capacity. However, inspite of this result, AP vendors may choose to support greater number of STAs on simultaneous DL as that may be independently desirable [2]. It is noteworthy that codebook info 1 (i.e., using more bits to quantize the V-matrix) always has lower effective channel capacity performance than codebook info 0 in Fig 3. This is because we assume the perfect channel estimation which does not produce channel estimation error under both Codebook info 0 and 1. Thus codebook info 1 with larger CSI overhead always suffers more than codebook info 0.

III. FACTOR 2: SPATIAL CORRELATION

In this section, we investigate the impact of spatial correlation on the SU and MU performance in practical environmental conditions. The spatial correlation among user's is characterized by two key factors: user separation, and distance between AP and STAs. We use the Shannon channel capacity (without CSI overhead) as the metric to investigate the SU and MU throughput as a function of spatial correlation next.

A. Clustered-based multi-path channel model

We use the class of *cluster-based multipath fading channels* to model the practical environmental conditions for indoor Wi-Fi downlink operation. Such models were introduced by Saleh and Valenzuela, and extended/elaborated upon by many other researchers [14]. In particular, IEEE 802.11ax indoor channel model [11] is a typical cluster-based channel model that we have adapted by incorporating a parameter for user separation, as shown in Fig. 4. IEEE 802.11ax indoor channel model represents the propagation environment as a collection of scatterers grouped into clusters, where each cluster represents objects in the vicinity that act as a forward scattering source of rays that reach the receiver. Such clusters are typically represented via spatio-temporal models that capture the spatial characteristics of the environment, such as the transmit/receive antenna correlation and the distribution of objects, etc.

A particular impact on our results arises from distinction between Line-of-sight (LoS) and Non-line-of-sight (NLoS)

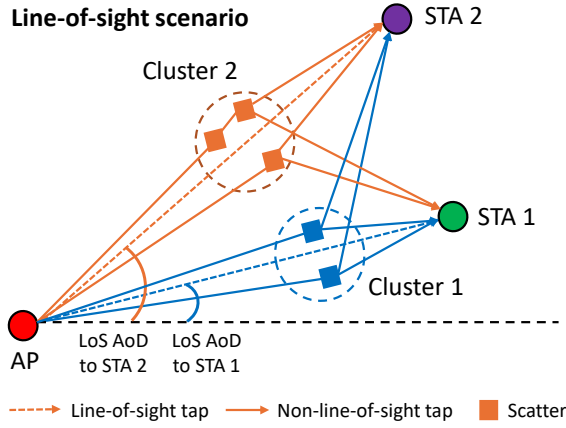


Fig. 4: DL SU (STA 1) and MU (STA 1 + 2) in Line-of-sight Scenario under Adapted IEEE 802.11ax Indoor Channel Model.

scenarios as defined by 11ax channel model specification, depending on the relationship between the breakpoint distance⁸ and the AP-STA separations [11]:

- *LoS scenario* (Fig. 4) occurs if the distance between AP and STAs is smaller than the breakpoint distance. The received signal at each STA include a LoS component and multiple multipath-induced NLoS components within a tapped delay-line model. This results in Rician fading multipath models where the first tap (corresponding to earliest arrival at each STA) is the LoS component. Therefore, the CSI obtained at each STA in such cases includes both LoS component and NLoS components with spatial characteristics [11]; LoS CSI component depends on the transmit/receive steering vector parameterized by LoS angle of departure (AoD)/angle of arrival (AoA). Each NLoS CSI component depends on transmit/receive antenna correlation parameterized by NLoS mean AoD/AoA along with angular spread, and the spatial distribution of random scatterers within the cluster. The mathematical expression for LoS/NLoS CSI components can be found at [15]. Since the first LoS tap signal is typically significantly stronger than NLoS signals, the LoS CSI component dominates the CSI obtained at each STA.
- *NLoS scenario* occurs if the distance between AP and STAs is greater than the breakpoint distance; then the LoS tap signal at each STA in Fig. 4 is blocked. Thus, the received signals at each STA are all NLoS (hence Rayleigh fading) and the first NLoS tap signal's power is close to that of the other NLoS taps.

B. Spatial Correlation

Fig. 4 shows a two-cluster scenario including an 8 x 8 uniform linear array (ULA)-based AP and two 1 x 1 STAs. AP transmits to STA 1 if MU-MIMO is turned off and to both STA

⁸The distance that separates LoS and NLoS scenarios with different path loss exponents.

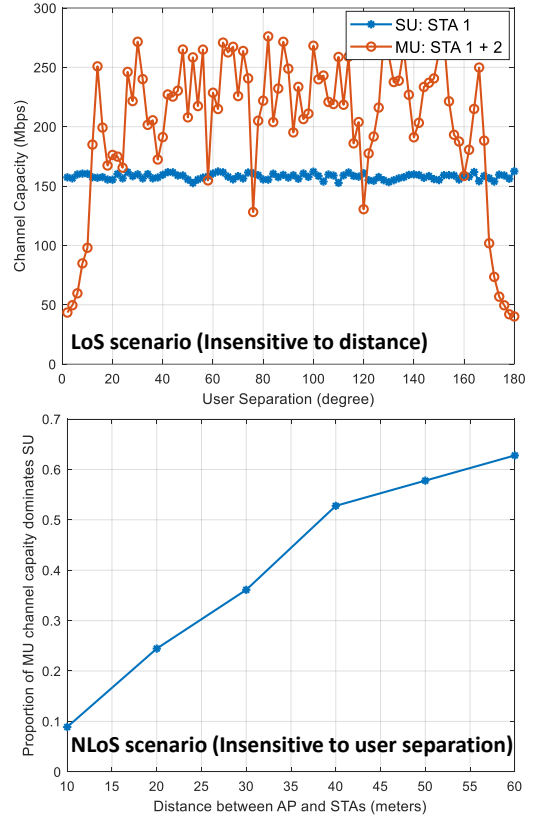


Fig. 5: Channel Capacity impacted by Spatial Correlation. 8 x 8 AP (ULA antenna spacing is half wavelength), 1 x 1 STAs, 20 dBm Transmit Power, 20 MHz Bandwidth, -174 dBm Noise Power Spectrum Density.

1 and STA 2 if MU-MIMO is turned on. The spatial geometry of STAs is characterized by their angle of departure (AoD), i.e., LoS AoD to STA 1 and LoS AoD to STA 2. The user separation between STA 1 and 2 is defined as the difference between LoS AoD to STA 2 and STA 1, respectively. To investigate the impact of user separation, we fix the angular geometry of cluster 1⁹ and STA 1, i.e., LoS AoD to STA 1 is set to 0° , and the LoS AoD to STA 2 varied between 0° and 180° , thus the user separation between STA 1 and 2 ranges between 0° and 180° .

1) *Dominant feature in the LoS scenario - User separation:* As the LoS distance is typically small due to the small breakpoint distance, e.g., within 10 meters, spatial correlation in the LoS scenario is not sensitive to the LoS distance variation. Thus user separation is the single dominant feature that we explore in the LoS scenario, which is shown in Fig. 5. Consider a set of LoS scenarios where the distance is 8 meters and the granularity of user separation is 2° , resulting in a total of 90 user separation scenarios. DL SU channel capacity dominates MU in 14% scenarios of which 12% scenarios lie in $0 - 12^\circ$ and $168 - 180^\circ$ user separation regions. Note that DL MU-MIMO channel capacity over $0 - 180^\circ$ user separation exhibits a symmetric channel capacity pattern, that

⁹Cluster 1's NLoS mean AoD equals the LoS AoD to STA 1; Cluster 2's NLoS mean AoD equals the LoS AoD to STA 2.

Factor 1: CSI Overhead			Factor 2: Spatial Correlation		Guideline
Number of STAs	Codebook Info for BF Compression	STA MIMO Dimension	Scenarios	User separation / Distance	Turn MU-MIMO ON or OFF
2	0	1 x 1	LoS (0 – 10 m)	0 – 15° and 165 – 180° user separation	OFF
				15 – 165° user separation	ON
			NLoS (10 – 60 m)	10 – 42 m distance	OFF
				42 – 60 m distance	ON
		2 x 2	LoS (0 – 10 m)	0 – 15° and 165 – 180° user separation	OFF
				15 – 165° user separation	ON
	NLoS (10 – 60 m)		10 – 52 m distance	OFF	
			52 – 60 m distance	ON	
	1	1 x 1	LoS (0 – 10 m)	0 – 15° and 165 – 180° user separation	OFF
				15 – 165° user separation	ON
			NLoS (10 – 60 m)	10 – 48 m distance	OFF
				48 – 60 m distance	ON
2 x 2		LoS (0 – 10 m)	0 – 15° and 165 – 180° user separation	OFF	
			15 – 165° user separation	OFF	
NLoS (10 – 60 m)	10 – 58 m distance	OFF			
	58 – 60 m distance	ON			

Fig. 6: Guideline Table for DL MU-MIMO with 8 x 8 AP under Adapted IEEE 802.11ax Channel Model.

can be attributed to the ULA characteristics where the LoS transmit/receive steering vectors of two STAs are identical at 0° or 180° user separation. Then, their dominant LoS CSI component determined by LoS transmit/receive steering vectors are also close for user separation regions close to 0° or 180° . As a result, the corresponding V-matrices become highly correlated, incurring significantly higher inter-user interference than other user separation regions.

2) *Dominant feature in the NLoS scenario - Distance between AP and STAs:* In the NLoS scenario, the obtained CSI includes only NLoS components, and each NLoS component (corresponding to a NLoS tap) is determined by the transmit/receive antenna correlation as well as the characteristics of scatterers. Since the latter such as their distributions, shapes and properties of materials are random, each NLoS tap consists of superposition of multiple independent individual path components leading to the complex Gaussian assumption [11]. As a result, the inter-user/inter-stream interference can vary significantly as a function of STA distance in such cases (and is insensitive to user angular separation).

The spatial correlation as a function of distance in NLoS is shown Fig. 5 for scenarios where the granularity of distance is 10 meters; the maximum distance for DL MU-MIMO operation with sufficiently high SNR at the STA is 60 meters. For each distance, 60 equally spaced user separations is used to calculate the proportion of scenarios in which MU channel capacity dominates SU. As shown, the proportion increases when distance increases, indicating that DL MU-MIMO benefits more than SU-MIMO at larger distance. In particular, MU becomes dominant over 50% scenarios for distances greater than 38 meters. The larger the distance is, the more the multiple scattering, reflection, and diffraction paths that decorrelate the signals received by different users.

Hence, the inter-user interference is effectively reduced with the increasing distance.

IV. DESIGN GUIDELINE FOR DL MU-MIMO

We now provide some practical design guidelines for DL MU-MIMO operation with 8 x 8 AP based on the effective channel capacity that unifies the underlying factors discussed in Section II and III. For the same setup as Fig. 5 used to obtain the channel capacity is now modified to derive the *effective* channel capacity as in Fig. 3. All results were implemented in Matlab using indoor MIMO WLAN channel models created by Schumacher et al, [15]. Due to page limits, we only provide guidelines for the 2-user case; this will be extended to cover other typical operational scenarios and reported elsewhere. Investigating more users results in more complicated scenarios to be categorized (e.g., a 3-user case will be characterized by 3 different user separations between each pair of users) and is left for future research work.

As the main features regarding CSI overhead are codebook information for BF compression (i.e., codebook info 0 and 1) and STA MIMO dimensions (i.e., 1 x 1 and 2 x 2 STA), there are a total of 4 different operational scenarios regarding CSI overhead. Meanwhile, spatial correlation is characterized by 2 typical user separation regions for LoS scenario, while it is characterized by 2 typical distance regions in the NLoS scenario. Thus there are also a total of 4 different operational scenarios regarding spatial correlation. As a result, we provide guidelines for 16 scenarios unifying both CSI overhead and spatial correlation, as shown in Fig. 6. Our conclusion for the 2-user case is that among these 16 scenarios, DL MU-MIMO can be turned on in 7 (43.75%). According to the guideline table, **DL MU-MIMO can be turned on in the following scenarios:**

- **1 x 1 STAs with sufficient user separation in LoS;**
- **2 x 2 STAs with codebook info 0 and sufficient user separation in LoS;**
- **Sufficiently large distance in NLoS.**

Otherwise, DL MU-MIMO is suggested to be turned off, i.e., switch to DL SU-MIMO. Note that the condition for turning on DL MU-MIMO is more stringent for the 2 x 2 STA case, compared to the 1 x 1 STA case. This is because each spatial stream in the 2 x 2 STA case suffers more from interfering streams (self-interference from another stream for same STA and/or streams from another STA) than the 1 x 1 STA case (only one interfering streams from another STA). Thus compared to the 1 x 1 STA case, MU-MIMO effective channel capacity is less likely to exceed SU-MIMO in the 2 x 2 STA case.

V. CONCLUSION

This article provides new insights about the key underlying factors (i.e., CSI overhead and spatial correlation) that have resulted in AP vendors turning off the DL MU-MIMO feature as the default setting in their products. Based on our study and analysis, guidelines as a function of operational scenarios is provided to address the fundamental question “when DL MU-MIMO should be turned on/off” for current/next-generation Wi-Fi systems.

REFERENCES

- [1] “IEEE Standard for Information Technology–Telecommunications and Information Exchange between Systems Local and Metropolitan Area Networks–Specific Requirements Part 11: Wireless LAN Medium Access Control (MAC) and Physical Layer (PHY) Specifications Amendment 1: Enhancements for High-Efficiency WLAN,” *IEEE Std 802.11ax-2021 (Amendment to IEEE Std 802.11-2020)*, pp. 1–767, 2021.
- [2] Cisco Meraki, “Wi-Fi 6 (802.11ax) Technical Guide,” 2023.
- [3] Qualcomm, “802.11ac MU-MIMO: Bridging the MIMO Gap in Wi-Fi,” 2015.
- [4] Signals Research Group, “MU-MIMO and the user experience,” 2016.
- [5] Arista Networks, “Multi-User MIMO in Wi-Fi 6 technical white paper,” 2013.
- [6] Cambium Networks, “802.11ax white paper 2020 vision on 802.11ax,” 2020.
- [7] H. Choi, T. Gong, J. Kim, J. Shin, and S.-J. Lee, “Use MU-MIMO at your own risk—Why we don’t get Gb/s Wi-Fi,” *Ad Hoc Networks*, vol. 83, pp. 78–90, 2019.
- [8] Extreme Networks, “Does the number of spatial streams in 802.11ax really matter?” 2017.
- [9] T. Higgins, “Why You Don’t Need MU-MIMO,” *SmallNetBuilder*, 2017.
- [10] S. Sur, I. Pefkianakis, X. Zhang, and K.-H. Kim, “Practical MU-MIMO user selection on 802.11 ac commodity networks,” in *Proceedings of the 22nd Annual International Conference on Mobile Computing and Networking*, 2016, pp. 122–134.
- [11] J. Liu, R. Porat, N. Jindal, V. Erceg, S. Azizi *et al.*, “IEEE 802.11 ax channel model document,” *Wireless LANs, Rep. IEEE*, pp. 802–11, 2014.
- [12] T. Yoo and A. Goldsmith, “On the optimality of multiantenna broadcast scheduling using zero-forcing beamforming,” *IEEE Journal on Selected Areas in Communications*, vol. 24, no. 3, pp. 528–541, 2006.
- [13] E. Björnson, M. Bengtsson, and B. Ottersten, “Optimal multiuser transmit beamforming: A difficult problem with a simple solution structure [lecture notes],” *IEEE Signal Processing Magazine*, vol. 31, no. 4, pp. 142–148, 2014.
- [14] T. S. Rappaport, *Wireless communications: principles and practice*. Cambridge University Press, 2024.
- [15] L. Schumacher and B. Dijkstra, “Description of a MATLAB implementation of the indoor MIMO WLAN channel model proposed by the IEEE 802.11 TGn channel model special committee,” *Implementation note version*, vol. 5, 2004.

Liu Cao received the B.E. degree in electrical engineering from Jinan University, Guangzhou, China, in 2017, and the M.S. degree in electrical engineering from Northwestern University, Evanston, IL, USA, in 2019. He is currently working toward the Ph.D. degree in electrical & computer engineering at the University of Washington, Seattle, WA, USA. His research interests include resource allocation in 5G NR Sidelink and Wi-Fi networks.

Lyutianyang Zhang received the B.E. degree in electronic communication from The Australian National University and the Beijing Institute of Technology in 2017 and the M.S. degree and Ph.D. Degree in electrical and computer engineering at the University of Washington in 2019 and 2023. His research interests include resource allocation problems, PHY-MAC cross-layer algorithm design, and simulator design for Wi-Fi, cellular systems, and mobile edge computing networks.

Sumit Roy received the B.Tech. degree in electrical engineering from the Indian Institute of Technology Kanpur in 1983, the M.S. and Ph.D. degrees in electrical engineering from the University of California, Santa Barbara Santa Barbara, CA, USA, in 1985 and 1988, respectively, and the M.A. degree in statistics and applied probability in 1988. He is currently a Professor with the Department of Electrical and Computer Engineering, University of Washington. His research interests include fundamental design and evaluation of wireless communication and sensor network systems spanning a diversity of technologies and application areas: next-gen (5G and beyond) wireless LANs and cellular networks, heterogeneous network coexistence, spectrum sharing, software-defined radio platforms, and vehicular and sensor networking. He was elevated as a fellow of IEEE by the Communications Society in 2007 for contributions to multi-user communications theory and cross-layer design of wireless networking standards.

Sian Jin received the B.E. degree in electronic information engineering from University of Electronic Science and Technology of China in 2016 and Ph.D. Degree in electrical and computer engineering at University of Washington in 2022. During 2022 spring and summer, he worked at Princeton University as a postdoc. Since 2022 fall, he has been working at MathWorks, developing state-of-the-art signal processing algorithms. His research interests include array processing, statistical signal processing, wireless localization, navigation and wireless communication.